Power Engineering and Engineering Thermophysics
https://www.acadlore.com/journals/PEET

Design of Greenhouse Ventilation Systems with Computational Fluid Dynamics: Balancing Performance and Energy Sustainability

Leila Riahinezhad[1], Ahmad Nooraeen[2*], Melika Mohammadkhah[3]

[1] Department of sustainability and energy, Mammut Group Company, 1513737511 Tehran, Iran
[2] Faculty of Biomedical Engineering, Amirkabir University of Technology, 1149754413 Tehran, Iran
[3] Institute of Mechanics, Technische Universität Berlin, 10623 Berlin, Germany

* Correspondence: Ahmad Nooraeen (nooraeen@aut.ac.ir)

Received: 04-12-2025 **Revised:** 06-10-2025 **Accepted:** 06-20-2025

Citation: L. Riahinezhad, A. Nooraeen, and M. Mohammadkhah, "Design of greenhouse ventilation systems with computational fluid dynamics: Balancing performance and energy sustainability," *Power Eng. Eng. Thermophys.*, vol. 4, no. 2, pp. 86–97, 2025. https://doi.org/10.56578/peet040201.

Abstract: Greenhouses are energy-intensive agricultural systems, where the sustainable design of natural ventilation could markedly reduce energy demand while maintaining optimal conditions for plant growth. The performance of natural ventilation arises from a multifaceted interaction among several determinants, including the geometric configuration of the greenhouse, prevailing environmental conditions, and the structural characteristics of ventilation openings and ducts. This study employed computational fluid dynamics (CFD) to assess the influence of roof inlet design on airflow distribution, regulation of canopy temperature, and energy performance in a single-span greenhouse measuring 20 × 10 × 6 meters. Six ventilation configurations were evaluated by varying the quantity and shape of roof inlets: three large inlets and ten smaller inlets, each with rectangular, oval, or circular geometries. The plant canopy was modeled as a porous medium to realistically capture aerodynamic resistance. Mesh independence was validated using outlet mass flux, and simulations were conducted under steady-state natural ventilation conditions. Key performance indicators included airflow velocity, temperature distribution, ventilation rate, wall shear stress (WSS), air changes per hour (ACH), and estimated annual energy saving. Results of the analysis revealed that circular and oval inlets enhanced air mixing and reduced thermal gradients within the canopy, whereas rectangular inlets generated localized recirculation zones and elevated WSS, resulting in lower energy efficiency. The inlet geometry and quantity played a critical role in the sustainable design of greenhouse ventilation. By integrating CFD-based airflow analysis with energy-saving assessments, this study offered a practical framework to guide greenhouse operators in optimizing ventilation strategies that balance productivity, thermal comfort, and long-term energy sustainability.

Keywords: Greenhouse ventilation; Natural ventilation design; Computational fluid dynamics (CFD); Optimization; Energy efficiency

1 Introduction

The global population growth and rising demand for food have emphasized the critical role of protected agriculture, particularly in controlled-environment greenhouses [1]. These structures provide a means to optimize crop yield and quality by offering protection from adverse weather conditions and pests, thus ensuring year-round production. However, the operational sustainability of modern greenhouses is significantly challenged by their high energy consumption [2], primarily driven by the need for precise climate control [3]. Conventional mechanical systems, such as fans and cooling pads, require substantial electricity and contribute to a large carbon footprint. In response, there has been a global push towards more sustainable and economically viable solutions [4]. Natural ventilation, which significantly reduces the reliance on mechanical systems, outperforms as a highly effective and passive method to regulate greenhouse climate by allowing passive heat and mass transfer [5]. This passive climate control mechanism in greenhouses not only lowers electricity costs but also minimizes carbon footprints, so as to align with global efforts towards energy-efficient and sustainable practices [6]. The efficiency of natural ventilation, however, is a complex interplay of various factors, including the geometric configuration of the greenhouse, its environmental conditions, and the design of ventilation openings and ducts. Optimizing this system is not merely

a consideration of design but a core strategy for transforming energy-intensive greenhouse operations into a more sustainable form of agriculture.

The study of natural ventilation in greenhouses has traditionally relied on empirical and experimental methods. These conventional approaches, such as physical models in wind tunnels and full-scale experiments using tracer gases, are often costly and time-consuming [7, 8]. They also present important practical challenges, including the difficulty of precisely measuring airflow and temperature distribution in every region of a large and complex environment. These limitations often restricted the quantity of design variations that could be tested, hence a slow and resource-intensive process for a comprehensive optimization. Computational fluid dynamics (CFD) has emerged as an invaluable tool for analyzing and optimizing airflow patterns in complex environments like greenhouses [9, 10]. Unlike traditional experimental methods, which are often expensive and laborious, CFD simulations provide a detailed visualization of air movement, temperature distribution, and mass transfer. This allows researchers to virtually test various design modifications and predict their impact on the overall performance of the ventilation system [11]. CFD-guided optimization has been successfully applied to improve natural ventilation by optimizing vent sizes, locations, and types to enhance thermal comfort for crops and reduce energy consumption [12, 13].

It has been highlighted that when energy-consuming devices such as fans, heating, and cooling systems are employed, the configuration and geometry of air ducts play a crucial role in system performance. A key aspect of effective natural ventilation is the design and shape of air ducts, which can significantly influence airflow resistance and overall system efficiency [14]. Rectangular ducts are widely used due to their ease of fabrication and installation, but they create higher pressure drops and greater turbulence, which can impede airflow [15]. Oval ducts, on the other hand, offer a compromise and provide lower airflow resistance than rectangular ducts, while being more adaptable for installation in confined spaces [16]. Circular ducts are considered the most aerodynamically efficient, as their smooth and curved shape minimizes pressure loss and turbulence [17]. To accurately model the greenhouse environment, the dense plant canopy should be taken into account. The plant acts as a significant obstacle to airflow; it increases drag and redistributes the air within the greenhouse [18]. These effects could be precisely captured when researchers model the plant canopy as a porous medium by assigning specific hydraulic resistance properties to the crop volume [19]. This approach provides a realistic representation of how plants influence the microclimate, hence enabling more accurate predictions of temperature distribution and ventilation efficiency.

Despite extensive research on greenhouse ventilation, a significant gap remains in the systematic optimization of duct shape and quantity, particularly for natural ventilation systems. Most existing studies have focused on a single duct shape or a limited set of configurations, leaving substantial room for performance improvements unexplored. This study addressed that gap by conducting a comprehensive and CFD-guided optimization of duct geometry and quantity for enhanced efficiency of natural ventilation. Besides, this research investigated the impact of circular, oval, and rectangular duct shapes and quantities on the efficiency of natural ventilation and their associated energy saving in greenhouses. The primary objective is to identify the optimal duct configuration that maximizes airflow and thermal uniformity, while effectively reducing energy consumption. Performance was assessed through simulations that evaluated the effect of each design on crop thermal comfort and overall temperature distribution within the greenhouse. By systematically varying duct parameters, the most effective design was determined to cater for specific greenhouse geometries and climatic conditions. This comprehensive CFD-guided analysis is expected to highlight configurations that offer substantial cost saving and promote more sustainable greenhouse operations.

2 Materials and Methods

This section presents the physical model, computational setup, and methodology employed in CFD simulations. Additionally, the validation procedures are outlined to ensure the reproducibility and reliability of the simulation results.

2.1 Greenhouse Geometry, Vegetation, and Duct Configurations

Figure 1a provides a comprehensive overview of the geometric model. Figure 1a illustrates the computational domain, which features a single-span greenhouse measuring 20 m in length, 10 m in width, and 6 m in height. The internal volume includes a simulated plant canopy, modeled as a porous medium with dimensions of 18 m × 8 m × 2 m and positioned at ground level. The model incorporated a natural ventilation system consisting of four outlets, each with a cross-sectional area of 1 × 3 m^2, symmetrically located on the opposing sidewalls. Figure 1b presents a visual summary of six investigated configurations of distinct roof inlets. Two primary scenarios were considered: 1) a high-count inlet configuration with ten smaller ducts (R10, O10, and C10), each having a cross-sectional area of 3 m^2; 2) A low-count configuration with three larger ducts (R3, O3, and C3), each with a cross-sectional area of 10 m^2. For both scenarios, three different duct shapes were analyzed: rectangular (R), oval (O), and circular (C). This systematic variation in shape and quantity allows a detailed comparative analysis of their influence on ventilation performance.

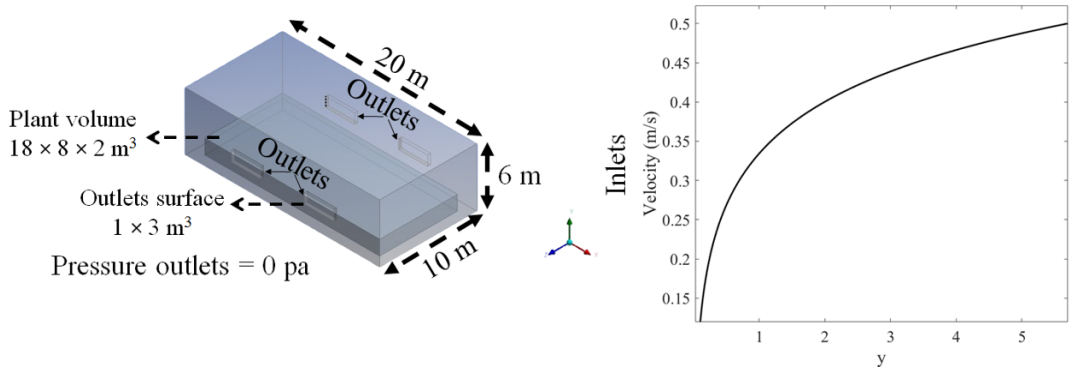

(a)

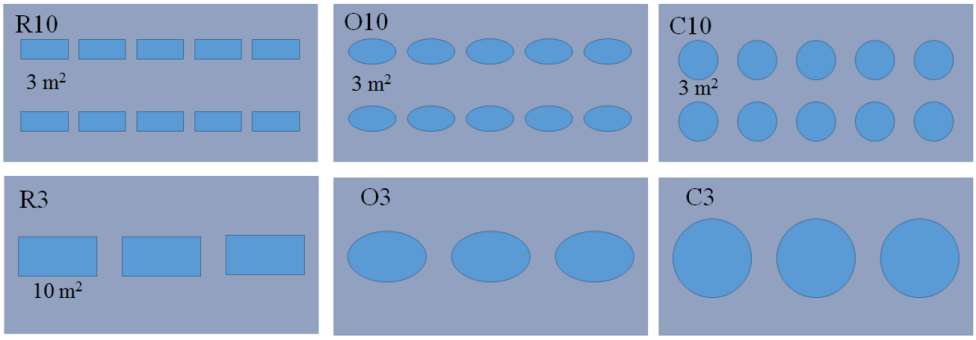

(b)

Figure 1. Geometric model and ventilation configurations of the simulated greenhouse: (a) Computational domain of a single-span greenhouse (20 × 10 × 6 m^3) with a porous plant canopy layer (18 × 8 × 2 m^3) and four sidewall outlets (1 × 3 m^2 each). Moreover, the inlet and outlet boundary conditions are introduced; (b) Two configurations of roof inlets. i) Comparing ten small inlets (R10, O10, and C10, 3 m^2 each). ii) Three large inlets (R3, O3, and C3, 10 m^2 each) with rectangular, oval, and circular duct shapes

2.2 Computational Fluid Dynamics Simulations and Governing Equations

In CFD simulations, the air was modeled as an incompressible fluid, with a constant density assumption at standard atmospheric conditions.

The steady-state flow field was simulated using ANSYS Fluent 16.1, based on the governing equations of continuity, momentum, and energy. Airflow was modeled using the Reynolds-Averaged Navier-Stokes equations. The shear stress transport k–ω model was employed due to its proven accuracy in predicting separated and swirling flows, rendering it appropriate for the complex geometry and flow behavior characteristic of naturally ventilated greenhouses [20]. The governing equations for mass, momentum [21], and energy are as follows:

$$\frac{\partial\left(\rho u_{\mathrm{i}}\right)}{\partial x_{\mathrm{i}}}=0 \tag{1}$$

$$\frac{\partial\left(\rho u_{\mathrm{i}} u_{\mathrm{j}}\right)}{\partial x_{\mathrm{j}}}=-\frac{\partial P}{\partial x_{\mathrm{i}}}+\frac{\partial}{\partial x_{\mathrm{j}}}\left[\mu\left(\frac{\partial u_{\mathrm{i}}}{\partial x_{\mathrm{j}}}+\frac{\partial u_{\mathrm{j}}}{\partial x_{\mathrm{i}}}\right)\right]+\frac{\partial \tau_{\mathrm{i}\,\mathrm{j}}}{\partial x_{\mathrm{j}}}+\rho g_{\mathrm{i}} \tag{2}$$

$$\frac{\partial\left(\rho u_{\mathrm{i}} h\right)}{\partial x_{\mathrm{j}}}=\frac{\partial}{\partial x_{\mathrm{j}}}\left[k_{\mathrm{eff}} \frac{\partial T}{\partial x_{\mathrm{j}}}\right]+S_{\mathrm{h}}+\rho u_{\mathrm{j}} g_{\mathrm{i}} \tag{3}$$

Here, ρ denotes the fluid density, u_{i} is the velocity component, P represents the static pressure, and μ is the dynamic viscosity of the fluid. The term τ_{ij} corresponds to the Reynolds stress tensor, while g_{i} indicates the body force component. The symbol h refers to the specific enthalpy, k_{eff} is the effective thermal conductivity accounting for both molecular and turbulent contributions, and S_{h} represents the volumetric source term associated with heat generation within the domain. Table 1 presents a list of constants incorporated for the simulation.

Table 1. List of constants used for the simulation [22]

Constant	Value (unit)
Fluid density	1.225 kg/m^3
Specific heat	1006.43 (J/(kg·K))
Thermal conductivity	0.0242 (W/(m·K))
Viscosity	1.7894e-05 (kg/(m·s))

2.3 Boundary Conditions and Meshing

The simulations were conducted using the following boundary conditions. The ground temperature was set to a constant 304 K, while the temperatures of the sidewalls and roof were maintained at 303 K. Airflow entering through the roof inlets was defined using a logarithmic velocity profile, a standard approach for modeling atmospheric boundary layers. This velocity profile, shown in Figure 1a, varies as a function of height (y) from the ground and was derived from a predefined atmospheric profile consistent with values reported in a previous study [23]. The outlet boundaries were assigned a pressure-outlet condition with a gauge pressure of 0 Pa. A comprehensive mesh independence study was conducted to ensure the accuracy and reliability of the simulation results. The mesh was refined iteratively, with mass flow rate at the outlets selected as the key parameter for convergence analysis. Mesh independence was achieved when the difference in mass flow between two consecutively finer meshes was less than 1%, to ensure that the simulation results were not influenced by mesh resolution. The computational domain was discretized using a tetrahedral mesh with an average element size of 100 mm.

The meshed geometry of the greenhouse is illustrated in Figure 2. The main panel displays the overall tetrahedral mesh applied to the computational domain, while the inset provides a close-up view of a specific region, thus highlighting the mesh quality and resolution. This figure supports the robustness of the mesh strategy and the credibility of the numerical analysis.

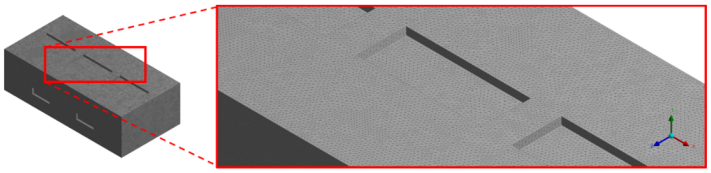

Figure 2. Computational mesh of the greenhouse domain. A tetrahedral grid with an average element size of 100 mm, followed by a mesh independence study based on outlet mass flow flux. The inset highlights a refined section of the mesh to confirm numerical stability and accuracy

2.4 Indicators of Ventilation Performance

This study provided an understanding of the impact of different duct shapes and quantities on key performance metrics relevant to greenhouse ventilation. The primary parameters analyzed included: velocity, temperature distribution, airflow streamlines, wall shear stress (WSS), ventilation rate, air changes per hour (ACH), and annual energy saving.

Temperature distribution, which directly affects crop health and productivity, is assessed to evaluate the uniformity of cooling or heating within the greenhouse. Airflow streamlines are used to visualize circulation patterns, revealing recirculation zones or dead spots that can diminish ventilation efficiency.

WSS serves as an indicator of energy losses and surface friction effects, while ventilation rate and ACH quantify air renewal, which is critical for maintaining optimal CO_2 levels and humidity control.

Ultimately, annual energy savings are estimated by comparing different duct configurations; this offers an economic assessment that links choices of ventilation design to long-term operational efficiency and sustainability.

3 Results

The analysis focused on key performance indicators, including velocity fields, temperature distribution, airflow streamlines, WSS, ventilation rate, energy saving, and ACH. These parameters allow a systematic comparison of six cases, to highlight the influence of duct geometry and quantity on the overall ventilation efficiency and thermal comfort inside the greenhouse.

3.1 Velocity Contour

In Figure 3, the magnitude of airflow within the greenhouse volume is illustrated at a vertical plane cross-section of the greenhouse, which is perpendicular to the inlet plane. The panels were organized into two groups: The top row displays the ten-inlet configurations (R10, O10, and C10), while the bottom row shows the three-inlet configurations (R3, O3, and C3). In all panels, the highest velocities are concentrated near the inlet openings. As the air moves into the greenhouse, its velocity decreases remarkably and the air transitions to the cooler areas. Comparing the different shapes, the panels for the circular (C10 and C3) and oval (O10 and O3) ducts show a more gradual and widespread velocity reduction within the greenhouse. In contrast, the panels for the rectangular ducts (R10 and R3) appear to have a slightly more abrupt velocity drop, with a more concentrated high-velocity zone at the inlets.

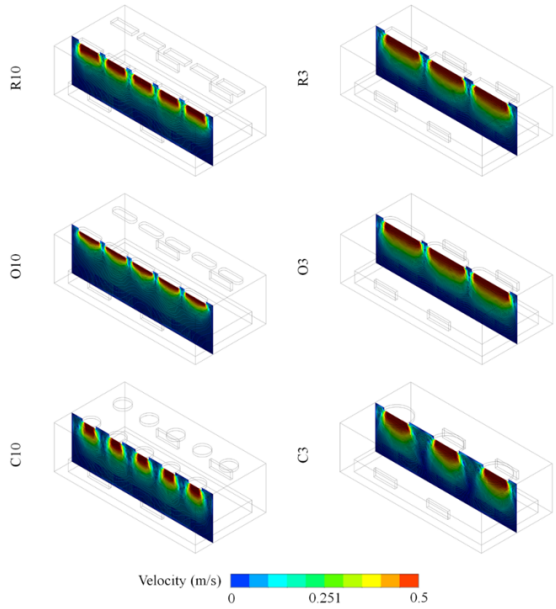

Figure 3. Velocity contour plots at the vertical plane of the greenhouse for six duct configurations (R10, O10, C10, R3, O3, and C3). Higher velocities were observed near the inlets, while gradual velocity decay occurred deeper inside the greenhouse

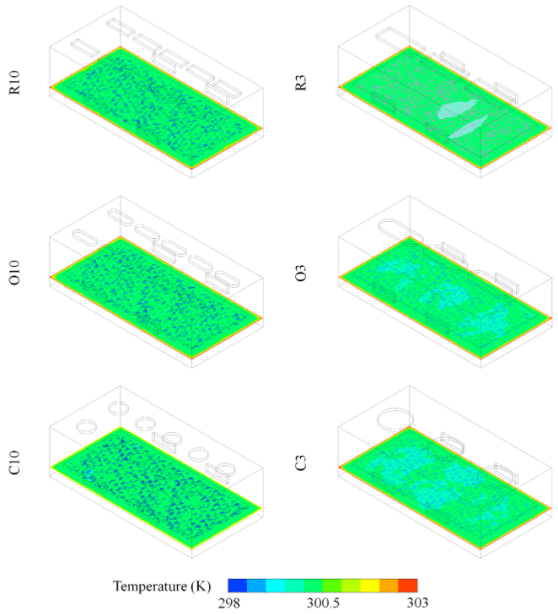

Figure 4. Temperature distribution on the plant canopy surface (298–303 K) of the six configurations. Circular and oval ducts exhibit relatively cooler canopy temperatures compared to rectangular ducts

3.2 Temperature Distribution

Figure 4 demonstrates the temperature distribution across the middle surface of the canopy for the six different ventilation configurations. The temperature was distributed relatively uniformly across the canopy for all configurations. Nevertheless, a closer examination revealed that the circular duct configurations (C10 and C3) exhibited more extensive regions of blue coloring, which signified a lower overall temperature on the plant canopy surface, compared to the rectangular duct configurations (R10 and R3). The latter indicates a higher prevalence of warmer areas owing to different duct configurations.

3.3 Airflow Streamlines

Figure 5 presents a three-dimensional visualization of airflow streamlines for each of the six duct configurations. These streamlines trace the complete airflow path from the inlets to the outlets, thus offering insight into internal circulation behavior. The rectangular configurations (R10 and R3) exhibit more pronounced localized swirling and recirculation zones near the inlet regions. In contrast, the circular (C10 and C3) and oval (O10 and O3) configurations display smoother and more direct flow paths throughout the greenhouse interior. This visualization underscores the significant influence of duct shape on airflow behavior, with smoother profiles promoting more uniform and efficient ventilation.

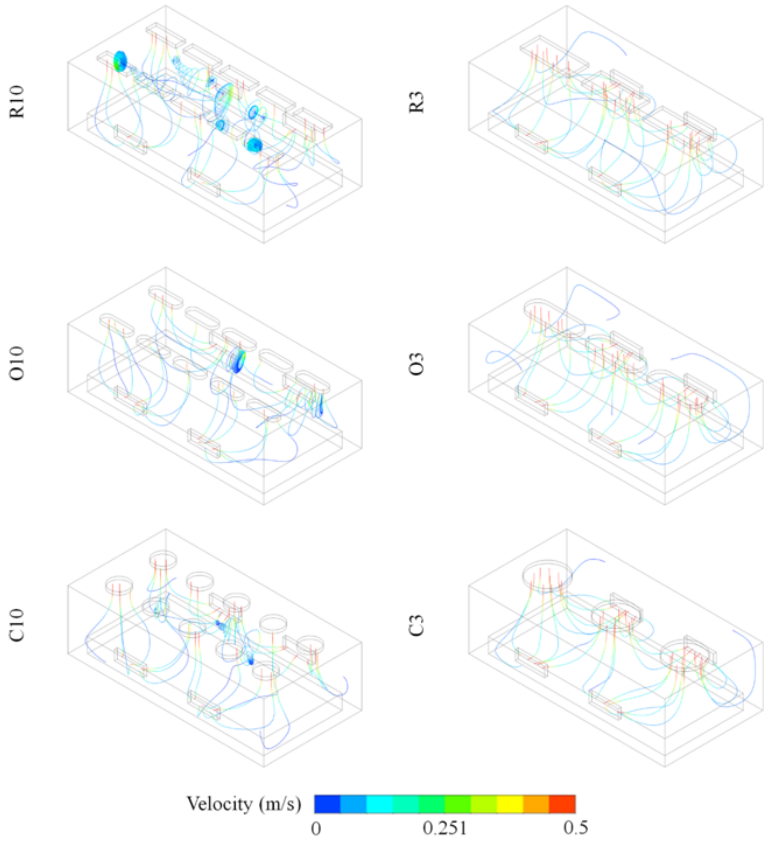

Figure 5. Three-dimensional airflow streamlines inside the greenhouse for the six duct designs. Rectangular ducts generate localized recirculation zones, while circular and oval ducts promote smoother flow paths

3.4 Wall Shear Stress Contour

Figure 6 illustrates the WSS contours with a color scale ranged from 0 to 283 × 10^{-6} Pa on the exterior surfaces of the greenhouse for all six duct configurations. WSS serves as a key indicator of frictional energy losses and the aerodynamic drag experienced by airflow along the surfaces. In all configurations, the highest WSS values were observed near the sharp edges and inlet openings, where flow separation and shear were most pronounced. A comparative analysis revealed that the rectangular ducts (R10 and R3) exhibited both larger high-WSS areas and higher WSS magnitudes than their circular (C10 and C3) and oval (O10 and O3) counterparts. This suggested that rectangular ducts generated greater frictional drag, thus reducing overall flow efficiency compared to shapes that are more streamlined.

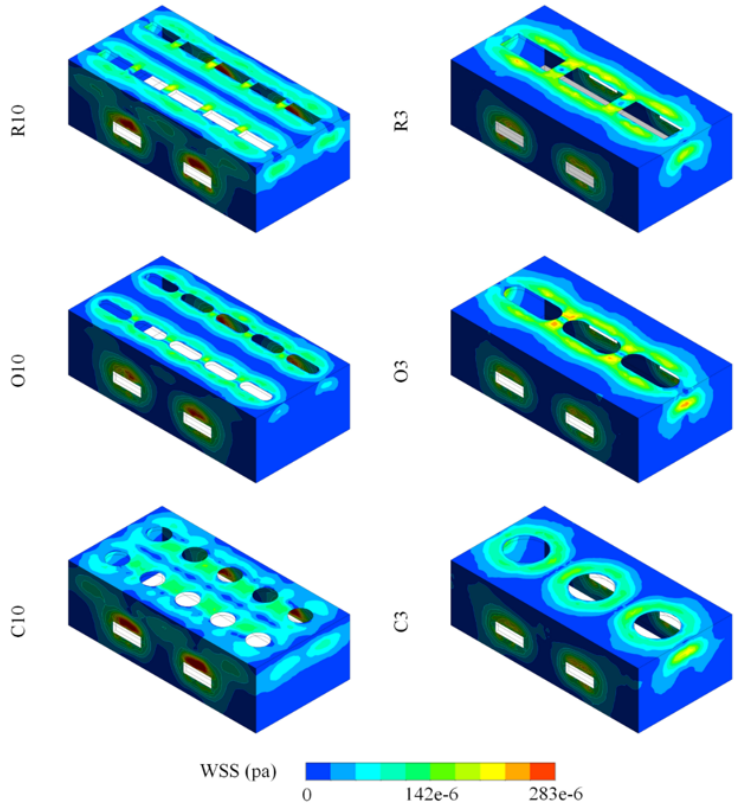

Figure 6. WSS distribution on the greenhouse surfaces for all configurations. Rectangular ducts exhibited higher frictional losses compared to circular and oval ducts

3.5 Energy Saving and Air Changes Per Hour

In Figure 7, the results demonstrate a trade-off between energy efficiency and ventilation capacity among the six duct designs. The left chart shows annual energy savings (in Joules) on the Y-axis, while the right chart shows the number of air changes per hour (ACH) on the Y-axis. The X-axis in both charts represents the different ceiling configurations. The results revealed that the R3 configuration saved the lowest amount of energy, whereas the C3 configuration conserved the highest amount. Additionally, the R3 and R10 configurations achieved the highest ACH, whereas the C10 configuration obtained the lowest ACH.

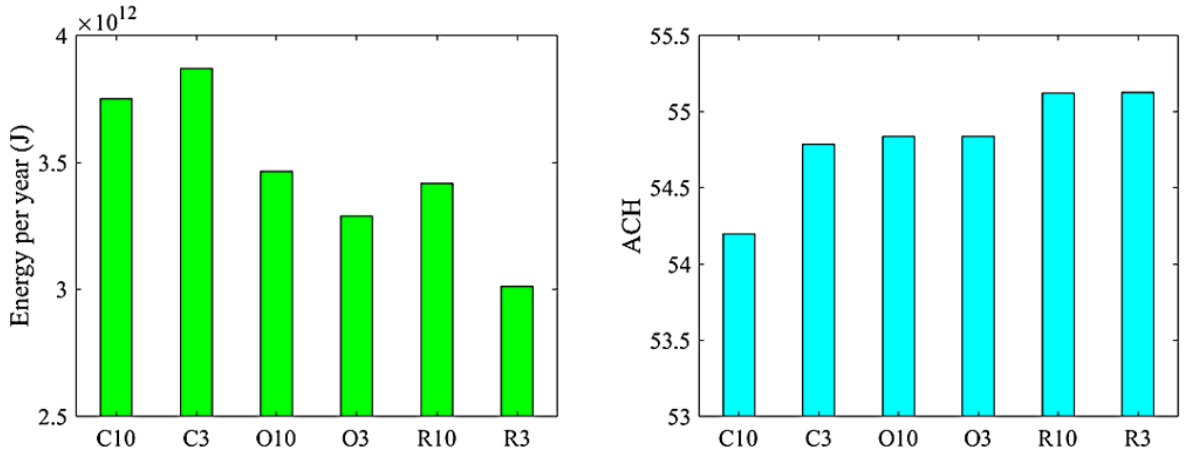

Figure 7. Comparative bar charts of total energy saving (Left), and ACH (Right)

3.6 Simulation Data of Flow, Temperature, and Power

Table 2 provides a numerical summary of the simulation results, with a breakdown of the corresponding values for mass flow rate, temperature of plant area, and power saving for the six configurations (R10, O10, C10, R3, O3, and C3). The mass flow rates are ranged from 18.066 kg/s for C10 to 18.375 kg/s for R3 and R10. The temperature of plant area shows a range from 297.427 K for C3 to 298.692 K for R3. Power saving in watts, varies significantly, with R3 having the lowest power consumption at 95 466.357 and C3 having the highest at 122 736.9075.

Table 2. Breakdown of the mass flow rate, temperature of plant area, and power saving for each duct configuration

Configuration	Mass Flow Rate (kg/s)	Temperature (K) of Plant Area	Power Saving (W)
R10	18.3749	298.109	108 385.1929
O10	18.2795	298.017	109 850.6187
C10	18.066	297.539	118 982.0618
R3	18.375	298.692	95 466.357
O3	18.2797	298.267	104 340.491
C3	18.2616	297.427	122 736.9075

4 Discussion

This research offered a systematic and integrative evaluation of greenhouse ventilation by concurrently examining multiple interdependent parameters, including velocity distribution, thermal regulation, WSS, energy consumption, and air change rates. In contrast to prior studies that have typically considered these factors in isolation, the present work provided a holistic framework that captured the coupled influence of aerodynamic and thermal behaviors on ventilation efficiency. Furthermore, three distinct duct geometries, i.e., rectangular, circular, and oval, were investigated across different inlet configurations, thus representing the first comparative assessment of its kind. This multi-faceted approach highlighted the critical role of duct design in optimizing greenhouse microclimates while simultaneously advancing energy-efficient and sustainable operation strategies.

Velocity fields for the six duct configurations in Figure 3 highlighted how duct geometry and quantity influenced airflow penetration. The rectangular ducts of R10 and R3 exhibited localized high-velocity regions near the inlets, which rapidly decayed into stagnant zones. This behavior has been mentioned in previous studies, where sharp-edged openings generated stronger entrance jets but poorer overall mixing [24]. By contrast, the circular and oval ducts (C10, O10, C3, and O3) distributed velocity more uniformly across the greenhouse; this improved canopy ventilation and reduced dead zones. Such smoother velocity attenuation could promote better microclimate regulation and gas exchange at the plant level [25]. An investigation into multi-chapel greenhouses discovered that combining roof and side wall vents with different opening layouts, particularly when vent shapes were smooth rather than sharp-edged, resulted in significantly more uniform airflow distribution and reduced hot spots inside the canopy [26]. Environmental Monitoring and CFD Simulations in another study reported that roof vent placement and shape influenced not only the magnitude of airflow, but also the downstream mixing and microclimate uniformity under natural ventilation [27]. These studies supported our findings that circular and oval ducts outperformed rectangular designs in terms of velocity decay and dead-zone reduction. However, in the arched greenhouse case, some configurations with large rectangular vents under high external wind showed better air change rates, thus implying that rectangular vents may retain their merits in specific climatic or wind conditions [28].

The temperature contours, as shown in Figure 4, indicated relatively uniform conditions across all duct designs, but with distinct differences in canopy cooling efficiency. The circular duct configurations (C10 and C3) yielded noticeably cooler canopy temperatures, consistent with the enhanced airflow distribution observed earlier. Prior work emphasized that improved mixing and reduced stratification could lower canopy temperature, thereby enhancing photosynthetic efficiency and yield [29]. In contrast, rectangular ducts (R10 and R3) demonstrated warmer localized areas which could potentially increase thermal stress for plants. This outcome aligned with findings about the crucial impact of duct geometry on microclimate uniformity in greenhouse environments [5]. Modifying roof shape to improve air circulation led to significantly lower maximum canopy temperatures in sweet pepper greenhouses, in parallel to the advantage witnessed in the case of circular ducts in the current study [30]. Similarly, the semi-closed study of greenhouses demonstrated that combining cooling ducts with carefully placed vents reduced hot spots and improved average thermal comfort within the crop canopy [31]. In contrast, research suggested that when canopy height was tall ($\approx$ 1.8 m), even large side vent openings yielded less cooling benefit possibly due to reduced wind penetration deeper into the canopy; this explained the underperformance of rectangular ducts relative to rounded ones in certain scenarios [32]. On the other hand, a study discovered larger discrepancies of temperature in configurations with non-uniform vent layout or occluded flow paths, hence indicating that flow path obstruction by canopy or by geometry could degrade thermal uniformity [33]. These comparisons affirmed that duct shape (rounded versus

sharp-edged), quantity of inlets, and canopy height are critical in modulating cooling efficiency. When designing for thermal comfort and energy saving, the findings in this study suggested that circular or oval ducts provided a superior trade-off, especially where tall crop canopy or obstructed airflow might reduce the effectiveness of ventilation in rectangular designs.

The rectangular ducts generated more pronounced swirling zones close to the inlet edges, indicative of flow separation due to sharp corners (see Figure 5). Such recirculation could trap heat and humidity, thus leading to non-uniform microclimates as observed in experimental studies of greenhouse ventilation [34]. Similarly, a study reported that sharp-edged ducts in greenhouses led to less uniform airflow and increased thermal stratification [35]. Conversely, circular and oval ducts allowed smoother airflow trajectories with fewer vortices, which enhanced the renewal of indoor air. This observation corresponded with CFD analyses, which showed that rounded duct inlets reduce turbulence intensity and promote energy-efficient ventilation [36, 37].

Figure 6 quantifies WSS patterns, reflecting energy dissipation through duct–air interactions. The rectangular ducts present higher and more extensive WSS regions around inlet edges, consistent with their sharper geometry. This indicated greater frictional drag and higher energy losses, which negatively affected overall system efficiency. By comparison, the circular and oval ducts exhibited significantly lower WSS, thus reinforcing their advantage in reducing frictional losses. This supported the notion that smoother duct geometries not only improve airflow distribution but also extend duct durability and reduce long-term maintenance costs.

As shown in Figure 7, while the R3 and R10 configurations achieve the highest ACH, their energy savings are the lowest, highlighting a trade-off between ventilation capacity and energy efficiency. Similar findings reported that higher ACH did not necessarily translate into optimal energy use [38]. Conversely, the circular duct configurations, particularly the C3, achieve the highest energy saving while maintaining satisfactory ACH. This balance between ventilation and cost aligned with sustainable greenhouse management strategies, which prioritize reduced energy consumption without compromising crop health [38]. Based on these findings, product shape is proved to be strongly conducive to both economic and environmental outcomes.

The circular ducts (C3 and C10) consistently produced lower canopy temperatures; with the C3 reaching the coolest value of 297.427 K. These configurations exhibited higher power saving, particularly the C3 at 122 736 W, which significantly outperformed the rectangular ducts (see Table 2). Although rectangular ducts (R3 and R10) allowed slightly higher mass flow rates, they corresponded to higher plant temperatures and lower energy efficiency. This pattern was consistent with earlier CFD-based evaluations of greenhouse ventilation, where duct geometry dictated the balance between airflow rate and energy performance [22]. Consequently, the data reinforced that rounded duct geometries were more advantageous for balancing climate control, crop comfort, and cost-effectiveness.

Despite the comparative analysis performed in this study, several limitations should be acknowledged. First, the simulations assumed steady-state boundary conditions and neglected transient environmental variations, such as diurnal changes in solar radiation, external wind fluctuations, and seasonal temperature shifts, which can significantly influence greenhouse microclimates. Second, the plant canopy was modeled as a homogeneous porous medium, which simplified the complex aerodynamic interactions between individual leaves and stems. This model of plant canopy may lead to discrepancies when predicting localized airflow patterns and heat transfer near plant surfaces. Additionally, the thermal properties of the greenhouse materials were considered constant, when possible variations were ignored due to aging or moisture content. Future work should aim to implement fully transient CFD and fluid-structure interaction (CFD- Fuel Stratified Injection) simulations with dynamic environmental inputs to capture real-world ventilation performance. Incorporating detailed plant morphology and leaf-level turbulence modeling could further improve the accuracy of microclimate predictions. Finally, experimental validation in operational greenhouses would strengthen the reliability of the numerical findings and allow refinement of model parameters for broader applications.

5 Conclusions

The present study thoroughly examined the role of duct geometry and quantity in enhancing the efficiency of greenhouse ventilation system. By analyzing airflow patterns, temperature distribution, WSS, and overall energy performance, the research highlighted how variations in duct design could substantially influence both the microclimatic conditions and the energy demands of greenhouses. The comparative evaluation of different duct geometries revealed notable differences in their aerodynamic and thermal performance, as summarized below:

Circular and oval ducts generally:

- Promoted smoother airflow streamlines;
- Reduced recirculation zones;
- Achieved more uniform temperature distributions across the canopy.

Rectangular ducts were associated with:

- Localized high-velocity regions;
- Elevated WSS values;

• Greater frictional losses, leading to reduced energy efficiency.

Among all configurations tested, the C3 (circular, 3 inlets) was the most energy-efficient and it offered the highest power saving while maintaining favorable thermal conditions. The R3 (rectangular, 3 inlets) demonstrated less effective temperature control and lower energy efficiency, despite a high air change rate. These results underscored the importance of geometric optimization in natural ventilation systems and the balance of airflow uniformity, energy consumption, and thermal comfort at the crop level. Circular ducts were particularly advantageous when long-term operational costs and plant health were prioritized. Overall, this study provided valuable insights for designing energy-efficient greenhouse ventilation system, a reference framework for future experimental validation and large-scale implementation.

Data Availability

The data used to support the research findings are available from the corresponding author upon request.

Conflicts of Interest

The authors declare no conflicts of interest.

References

[1] C. Vatistas, D. D. Avgoustaki, and T. Bartzanas, "A systematic literature review on controlled-environment agriculture: How vertical farms and greenhouses can influence the sustainability and footprint of urban microclimate with local food production," *Atmosphere*, vol. 13, no. 8, p. 1258, 2022. https://doi.org/10.3390/atmos13081258

[2] W. Zhang, L. Li, and Y. Li, "Natural ventilation and energy consumption research for dry sports halls within national fitness centers in cold regions—Case study of Qingdao," *Buildings*, vol. 15, no. 5, p. 734, 2025. https://doi.org/10.3390/buildings15050734

[3] S. Boyacı, J. Kocięcka, B. Jagosz, and A. Atılgan, "Energy efficiency in greenhouses and comparison of energy sources used for heating," *Energies*, vol. 18, no. 3, p. 724, 2025. https://doi.org/10.3390/en18030724

[4] M. O. K. Azad, N. S. Gruda, and M. T. Naznin, "Energy efficiency of glasshouses and plant factories for sustainable urban farming in the desert southwest of the United States of America," *Horticulturae*, vol. 10, no. 10, p. 1055, 2024. https://doi.org/10.3390/horticulturae10101055

[5] M. C. Singh, K. K. Sharma, and V. Prasad, "Impact of ventilation rate and its associated characteristics on greenhouse microclimate and energy use," *Arab. J. Geosci.*, vol. 15, no. 3, p. 288. https://doi.org/10.1007/s12517-022-09587-1

[6] I. Gil-Ozoudeh, O. Iwuanyanwu, A. C. Okwandu, and C. S. Ike, "The role of passive design strategies in enhancing energy efficiency in green buildings," *Eng. Sci. Technol. J.*, vol. 3, no. 2, p. 71–91, 2022.

[7] J. Soriano, A. C. G. Shiguemoto, and J. G. Vieira Neto, "Advances in methodologies to assess wind actions in plastic-covered greenhouses," *Sci. Agric.*, vol. 81, p. e20220276, 2024. https://doi.org/10.1590/1678-992X-2022-0276

[8] I. Lee, S. Lee, G. Kim, J. Sung, S. Sung, and Y. Yoon, "PIV verification of greenhouse ventilation air flows to evaluate CFD accuracy," *Trans. Am. Soc. Agric. Eng.*, vol. 48, no. 6, p. 2277–2288, 2005. https://doi.org/10.13031/2013.20091

[9] Y. D. Akenteng, H. Chen, K. N. Opoku, F. Ullah, S. Wang, and S. Kumar, "The role of computational fluid dynamics (CFD) in phytohormone-regulated microalgae-based carbon dioxide capture technology," *Sustainability*, vol. 17, no. 3, p. 860, 2025. https://doi.org/10.3390/su17030860

[10] J. Flores-Velazquez, J. I. Montero, E. J. Baeza, and J. C. Lopez, "Mechanical and natural ventilation systems in a greenhouse designed using computational fluid dynamics," *Int. J. Agric. Biol. Eng.*, vol. 7, no. 1, p. 1–16, 2014.

[11] L. Y. Choi, K. F. Daniel, S. Y. Lee, C. R. Lee, J. Y. Park, J. Park, and S. W. Hong, "CFD simulation of dynamic temperature variations induced by tunnel ventilation in a broiler house," *Animals*, vol. 14, no. 20, p. 3019, 2024. https://doi.org/10.3390/ani14203019

[12] S. Wangkahart, C. Junsiri, A. Srichat, K. Laloon, K. Hongtong, P. Boupha, S. Katekaew, and S. Poojeera, "Modeling airflow and temperature in a sealed cold storage system for medicinal plant cultivation using computational fluid dynamics (CFD)," *Agronomy*, vol. 14, no. 12, p. 2808, 2024. https://doi.org/10.3390/agronomy14122808

[13] S. Mazzetto, "Dynamic integration of shading and ventilation: Novel quantitative insights into building performance optimization," *Buildings*, vol. 15, no. 7, p. 1123, 2025. https://doi.org/10.3390/buildings15071123

[14] H. Benzzine, H. Labrim, A. Saad, Y. Achour, D. Zejli, and R. El Bouayadi, "Energy design and optimization of greenhouse by natural convection," *Fluid Dyn. Mater. Process.*, vol. 20, no. 8, p. 1903–1913, 2024. https://doi.org/10.32604/fdmp.2024.050557

[15] S. K. Saha, "Thermohydraulics of turbulent flow through rectangular and square ducts with axial corrugation roughness and twisted-tapes with and without oblique teeth," *Exp. Therm. Fluid Sci.*, vol. 34, no. 6, p. 744–752, 2010. https://doi.org/10.1016/j.expthermflusci.2010.01.003

[16] J. Menéndez, J. M. Fernández-Oro, M. Galdo, L. Álvarez, C. López, A. Bernardo-Sánchez, and M. B. D. Aguado, "Oval ducts in mining ventilation systems: Optimization of the operation costs and increase of clearance in mine roadways," *Mining, Metall. Explor.*, vol. 42, p. 557–570, 2025. https://doi.org/10.1007/s42461-025-01206-3

[17] N. Chiereghin, L. Guglielmi, A. M. Savill, T. Kipouros, E. Manca, A. Rigobello, M. Barison, and E. Benini, "Shape optimization of a curved duct with free form deformations," in *23rd AIAA Computational Fluid Dynamics Conference*, 2017, p. 4114. https://doi.org/10.2514/6.2017-4114

[18] C. R. Chu, T. W. Lan, R. K. Tasi, T. R. Wu, and C. K. Yang, "Wind-driven natural ventilation of greenhouses with vegetation," *Biosyst. Eng.*, vol. 164, p. 221–234, 2017. https://doi.org/10.1016/j.biosystemseng.2017.10.008

[19] X. Xue, M. Bu, Z. Li, Y. Li, Y. Liu, W. Ye, C. Huang, and S. Lyu, "Research on the application effect and parameter optimization of 3HW36 Mountain Orchard Rail-Mounted Wind-Driven Plant Protection Equipment in fruit tree canopy," *Agronomy*, vol. 15, no. 4, p. 781, 2025. https://doi.org/10.3390/agronomy15040781

[20] G. Partheniotis, S. D. Kalamaras, A. G. Martzopoulou, V. K. Firfiris, and V. P. Fragos, "Turbulence models studying the airflow around a greenhouse based in a wind tunnel and under different conditions," *AgriEngineering*, vol. 4, no. 1, p. 216–230, 2022. https://doi.org/10.3390/agriengineering4010016

[21] A. Nooraeen, F. Ghalichi, H. Taghizadeh, and R. Guidoin, "Probing the possibility of lesion formation/progression in vicinity of a primary atherosclerotic plaque: A fluid-solid interaction study and angiographic evidences," *Int. J. Numer. Method. Biomed. Eng.*, vol. 38, no. 7, p. e3605, 2022. https://doi.org/10.1002/CNM.3605

[22] T. Bartzanas, T. Boulard, and C. Kittas, "Effect of vent arrangement on windward ventilation of a tunnel greenhouse," *Biosyst. Eng.*, vol. 88, no. 4, p. 479–490, 2004. https://doi.org/10.1016/j.biosystemseng.2003.10.006

[23] M. F. P. Lopes, M. G. Gomes, and J. G. Ferreira, "Simulation of the atmospheric boundary layer for model testing in a short wind tunnel," *Exp. Tech.*, vol. 32, no. 4, p. 36–43, 2008. https://doi.org/10.1111/j.1747-1567.2007.00293.x

[24] T. Boulard and S. Wang, "Greenhouse crop transpiration simulation from external climate conditions," *Agric. For. Meteorol.*, vol. 100, no. 1, p. 25–34, 2000. https://doi.org/10.1016/S0168-1923(99)00082-9

[25] B. Cemek, A. Atiş, and E. Küçüktopçu, "Evaluation of temperature distribution in different greenhouse models using computational fluid dynamics (CFD)," *Anadolu J. Agric. Sci.*, vol. 32, no. 1, p. 54–54, 2017. https://doi.org/10.7161/omuanajas.289354

[26] A. Senhaji, M. Mouqallid, and H. Majdoubi, "CFD assisted study of multi-chapels greenhouse vents openings effect on inside airflow circulation and microclimate patterns," *Open J. Fluid Dyn.*, vol. 9, no. 2, p. 119–139, 2019. https://doi.org/10.4236/ojfd.2019.92009

[27] S. Benni, P. Tassinari, F. Bonora, A. Barbaresi, and D. Torreggiani, "Efficacy of greenhouse natural ventilation: Environmental monitoring and CFD simulations of a study case," *Energ. Build.*, vol. 125, p. 276–286, 2016. https://doi.org/10.1016/j.enbuild.2016.05.014

[28] H. Li, Y. Li, X. Yue, X. Liu, S. Tian, and T. Li, "Evaluation of airflow pattern and thermal behavior of the arched greenhouses with designed roof ventilation scenarios using CFD simulation," *PLoS One*, vol. 15, no. 9, p. e0239851, 2020. https://doi.org/10.1371/journal.pone.0239851

[29] M. Didion-Gency, A. Gessler, N. Buchmann, J. Gisler, M. Schaub, and C. Grossiord, "Impact of warmer and drier conditions on tree photosynthetic properties and the role of species interactions," *New Phytol.*, vol. 236, no. 2, p. 547–560, 2022. https://doi.org/10.1111/NPH.18384

[30] W. Limtrakarn, P. Boonmongkol, A. Chompupoung, K. Rungprateepthaworn, J. Kruenate, and P. Dechaumphai, "Computational fluid dynamics modeling to improve natural flow rate and sweet pepper productivity in greenhouse," *Adv. Mech. Eng.*, vol. 4, p. 158563, 2012. https://doi.org/10.1155/2012/158563

[31] J. C. Roy, H. Fatnassi, T. Boulard, J. B. Pouillard, and A. Grisey, "CFD determination of the climate distribution in a semi closed greenhouse with air cooling," *Acta Hortic.*, vol. 1170, p. 103–110, 2017. https://doi.org/10.17660/ActaHortic.2017.1170.11

[32] T. Bartzanas, N. Katsoulas, C. Kittas, T. Boulard, and M. Mermier, "The effect of vent configuration and insect screens on greenhouse microclimate," *Int. J. Vent.*, vol. 4, no. 3, p. 193–202, 2005. https://doi.org/10.1080/14733315.2005.12021990

[33] M. Hou, D. Xu, Z. Wang, L. Meng, L. Wang, Y. Ma, J. Zhu, and C. Lv, "Computational fluid dynamics simulation and quantification of solar greenhouse temperature based on real canopy structure," *Agronomy*, vol. 15, no. 3, p. 586, 2025. https://doi.org/10.3390/agronomy15030586

[34] T. Norton, J. Grant, R. Fallon, and D. W. Sun, "Assessing the ventilation effectiveness of naturally ventilated livestock buildings under wind dominated conditions using computational fluid dynamics," *Biosyst. Eng.*, vol. 103, no. 1, p. 78–99, 2009. https://doi.org/10.1016/j.biosystemseng.2009.02.007

[35] S. Sase, "Air movement and climate uniformity in ventilated greenhouses," *Acta Hortic.*, vol. 719, p. 313–323, 2006. https://doi.org/10.17660/actahortic.2006.719.35

[36] J. Ahn, E. M. Sparrow, and J. M. Gorman, "Turbulence intensity effects on heat transfer and fluid-flow for a circular cylinder in crossflow," *Int. J. Heat Mass Transf.*, vol. 113, p. 613–621, 2017. https://doi.org/10.1016/j.ijheatmasstransfer.2017.05.131

[37] A. Pakari and S. Ghani, "Airflow assessment in a naturally ventilated greenhouse equipped with wind towers: Numerical simulation and wind tunnel experiments," *Energ. Build.*, vol. 199, p. 1–11, 2019. https://doi.org/10.1016/j.enbuild.2019.06.033

[38] J. B. Campen and G. P. A. Bot, "Determination of greenhouse-specific aspects of ventilation using three-dimensional computational fluid dynamics," *Biosyst. Eng.*, vol. 84, no. 1, p. 69–77, 2003. https://doi.org/10.1016/S1537-5110(02)00221-0